Food and Chemical Toxicology 129 (2019) 444–457

Contents lists available at ScienceDirect

Food and Chemical Toxicology

journal homepage: www.elsevier.com/locate/foodchemtox

Cognitive-enhancing and ameliorative effects of acanthoside B in a scopolamine-induced amnesic mouse model through regulation of oxidative/inflammatory/cholinergic systems and activation of the TrkB/CREB/BDNF pathway

Govindarajan Karthivashan[a], Mee-Hyang Kweon[c], Shin-Young Park[a], Joon-Soo Kim[a], Deuk-Hoi Kim[c], Palanivel Ganesan[b], Dong-Kug Choi[a,b,*]

[a] Department of Applied Life Sciences, Graduate School of Konkuk University, Research Institute of Inflammatory Diseases, Chungju, 27478, Republic of Korea
[b] Department of Integrated Bio Science and Biotechnology, College of Biomedical and Health Science, Nanotechnology Research Center, Konkuk University, Chungju, 27478, Republic of Korea
[c] Research Center, Phyto Corporation, Seoul, 08826, Republic of Korea

ARTICLE INFO

Keywords:
Scopolamine
Amnesia
Anti-AChE
Antioxidant
Anti-inflammation
Salicornia europaea L
TrkB/CREB/BDNF

ABSTRACT

Recently, our research team reported the anti-amnesic potential of desalted-hydroethanolic extracts of *Salicornia europaea* L. (SE-EE). In this study, we performed bioactivity-guided isolation and identification of Acanthoside B (Aca.B), from SE-EE, as the potential bioactive candidate and examined anti-amnesic activity with its potential mechanism of action using an *in vivo* model. S7-L3-3 purified from SE-EE showed enhanced *in vitro* acetylcholinesterase (AChE) inhibitory activity. The isolated S7-L3-3 was identified and characterized as Aca.B using varied spectral analyses, i.e., Nuclear magnetic resonance (NMR), Ultraviolet–visible (UV–Vis), and Electrospray ionization-mass spectrometry (ESI-MS). In the *in vitro* studies, Aca.B exhibited negligible toxicity and showed a dose-dependent nitric oxide inhibitory potential in Lipopolysaccharide (LPS)-stimulated BV-2 microglial cells. In the *in vivo* studies, the oral administration of Aca.B to mice showed enhanced bioavailability and dose-dependent repression of the behavioral/cognitive impairment by regulating the cholinergic function, restoring the antioxidant status, attenuating the inflammatory cytokines/mediators and actively enriching neurotropic proteins in the hippocampal regions of the scopolamine-administered mice.

1. Introduction

Alzheimer's disease (AD), one of the most frequently reported chronic neurodegenerative complications, is typically characterized by a slow, irreversible, progressive loss of neuronal cells responsible for cognitive and memory capability, and it eventually poses a vast undesirable impact in performing the patient's day-to-day activities (Scheltens et al., 2016). According to a recent report from the World Alzheimer Report published by Alzheimer's Disease International (ADI), London, in 2018, approximately 50 million people worldwide had dementia AD, and the prevalence is expected to reach 88 million by 2050 (Patterson et al., 2018). In addition to the emotional distress faced by the family members and caregivers to take care of AD patients, in 2018, the monetary expenses for caregivers, medications and long-term hospice services for AD patients were estimated to be more than 277 billion dollars (Association, 2018). In the clinical pathology of AD, extracellular aggregate formation of amyloid-beta (Aβ) senile plaques and intracellular neurofibrillary tangle formation by hyperphosphorylated tau proteins are the two major hallmarks observed in brain autopsies of AD patients (Association, 2018; Ower et al., 2018). However, the neuronal cell death and progression of the disease conditions in AD patients is reportedly associated with a series of sequestered neuropathological events, i.e., deficiency of the acetylcholine system, excitotoxity, oxidative stress and neuroinflammation (Godyń et al., 2016; G Karthivashan et al., 2018a,b). Thus, recently, investigators have been momentously screening the pharmaceutical properties of several bioactive candidates by evaluating their wide therapeutic potential to curb these multifaceted neuropathological events associated

* Corresponding author. Department of Applied Life Sciences, Graduate school of Konkuk University, Research Institute of Inflammatory Diseases, Chungju, 27478, Republic of Korea.
E-mail addresses: karthivashan@gmail.com (G. Karthivashan), mhkweon@korea.ac.kr (M.-H. Kweon), ifresha@nate.com (S.-Y. Park), kgfdkr@gmail.com (J.-S. Kim), dhkim@phytoco.com (D.-H. Kim), palanivel67@gmail.com (P. Ganesan), choidk@kku.ac.kr (D.-K. Choi).

https://doi.org/10.1016/j.fct.2019.04.062
Received 19 March 2019; Received in revised form 29 April 2019; Accepted 30 April 2019
Available online 08 May 2019
0278-6915/

with AD pathology (Cong g Lee et al., 2018; Shal et al., 2018). Scopolamine, a muscarinic nonselective cholinergic inhibitor, is well known to inflict AD-like amnesic activities in animal models by generating substantial behavioral and cognitive impediments and the associated above-discussed biochemical alterations inclusive of oxidative stress and neuro-inflammation (Govindarajan Karthivashan et al., 2017; Van Dam and De Deyn, 2011). It is also noteworthy that accumulating evidence has suggested that scopolamine disturbs the molecular homeostasis of tropomyosin receptor kinase B (TrkB) and cAMP response element binding (CREB)/brain-derived neurotrophic factor (BDNF) pathways in animal models (F. Li, Gong, Wu, Lu and Shi, 2010; Min et al., 2015) and substantially mimics the events of CREB/BDNF impairments in AD pathogenesis in the human brain (Bartolotti et al., 2016). Thus, the scopolamine-induced classic AD-like amnesic model has been adapted in this study for therapeutic investigations.

Salicornia europaea L. (SE), a halophytic plant species, has been recently investigated for its wide substantial therapeutic properties (Rhee et al., 2009). Park et al. demonstrated the anti-diabetic potential of hydroethanolic extracts of SE in high-fat-diet-induced hyperlipidemic mice by potentially regulating the genes associated with lipogenesis (SREBP1a, FAS GAPT) in the liver (Park et al., 2006). Hwang et al. determined the anti-tumor invasive potential of 3,4-dicaffeoylquinic acid, isolated from the SE extract, by inhibiting Matrix Metalloproteinase-9 (MMP-9) expression and regulating the Activator protein 1 (AP-1) and Mitogen-activated protein kinases (MAPKs) signaling pathways (Hwang et al., 2010). Eventually, another research team described the neuroprotective effects of ethanolic extracts of SE and its methylene chloride fractions by potentially regulating the nuclear factor (erythroid-derived 2)-like 2 (Nrf2)/heme oxygenase 1 (HO-1) antioxidant system in glutamate-induced hippocampal HT22 cells (Kim et al., 2017). Recently, our research team demonstrated the anti-amnesic potential of the desalted and enzyme-digested SE ethanol extract (SE-EE) in a mouse model (Govindarajan Karthivashan et al., 2018a,b). As an extension of our previous works, in this study, we aimed to identify the potential bioactive candidate responsible for the enhanced therapeutic activities of SE-EE. Here, SE-EE was subjected to *in vitro* anti-AChE activity-guided purification, and the potential bioactive compound of SE-EE, S7-L3-3, was identified and characterized as Aca.B by using chromatographic and NMR techniques. The anticholinergic, antioxidative, anti-neuroinflammatory and anti-amnesic potential of Aca.B was further investigated and confirmed through a scopolamine-induced amnesic mouse model. To the best of our knowledge, we are the first to investigate and report the anti-cholinergic, anti-neuroinflammatory and anti-amnesic effects of Aca.B.

2. Material and methods

2.1. Materials

Scopolamine hydrochloride and tacrine hydrochloride hydrate were purchased from Sigma-Aldrich (St. Louis, MO, USA). Tween 80 was purchased from Calbiochem (Gibbstown, NJ, USA). A protease and phosphatase inhibitor cocktail in tablet form was obtained from Roche (Indianapolis, IN, USA). A 10× Radioimmunoprecipitation assay buffer (RIPA) buffer was procured from Millipore (Milford, MA, USA). All the other chemicals used were of high analytical grade obtained from Sigma, unless mentioned otherwise. Antibodies raised against inducible nitric oxide synthase (iNOS), cyclooxygenase-2 (COX-2), TrkB, phospho-TrkB (p-TrkB), β-actin and horseradish peroxidase-conjugated appropriate IgG secondary antibodies were purchased from Cell Signaling Technology, Inc. (Danvers, MA, USA). Specific antibodies raised against CREB, phospho-CREB (p-CREB), and BDNF were obtained from Abcam (Cambridge, UK). The polyvinylidene difluoride (PVDF) membrane was acquired from Millipore (Bedford, MA, USA). All the solvents used for isolation and chromatographic analysis were of analytical grade.

2.2. Preparation of the SE-EE

The desalted and enzyme-digested SE ethanol extract (SE-EE) was prepared with a cold-water extraction procedure and enzyme digestion methods as described previously (Govindarajan Karthivashan et al., 2018a,b). In brief, the desalted SE powder, also known as PhytoMeal (PM), was suspended in distilled water (1% pectinase/cellulose) and incubated for 15 h at 50 °C for enzyme-digestion and subsequently refluxed in ethanol (60%) for 3 h to obtain the residual SE-EE. Since the obtained residual extract is commercially termed as enzyme-digested PhytoMeal ethanol extract (PM-EE) by Phyto Corporation, here we refer to the same as enzyme-digested desalted *Salicornia europaea* L. ethanol extract (SE-EE) throughout the study for the reader's clarity.

2.2.1. In vitro anti-AChE activity-guided isolation of Aca.B

In vitro anti-AChE assay was adapted to screen the fractions and bioactive compounds and was measured by the spectrophotometric method developed by Ellman et al., with slight modifications, having acetylcholine iodide as substrates. The rate of thiocholine production is determined by the continuous reaction of the thiol with the 5,5-dithiobis-2-nitrobenzoate (DTNB) ion to produce the yellow anion of 5-thio-2-nitrobenzoic acid. The absorbance of the mixture was read at 412 nm at intervals of 30 s for 5 min, which was immediately followed by the addition of substrate, and then the percentage of inhibition was calculated.

The schema of anti-AChE activity-guided Aca.B isolation from SE-EE is shown in Fig. 1a. In brief, 20 g of SE-EE was dissolved in 5 L of distilled water and subjected to ethanol precipitation to eliminate high molecular polysaccharides and proteins. The obtained residue was filtered through Whatman No. 2 filter paper (Maidstone, England) and condensed using a rotary evaporator at 45 °C and freeze-dried. The lyophilizate was extracted with alkaline chloroform (pH-10) to obtain an alkaloidal fraction (SE-AL). A total of 2 g of this alkaloidal fraction was fractionated into 8 fractions (SE-S1, -S2, -S3, -S4, -S5, -S6, -S7, and -S8) using gradient solvent mixtures of $CHCl_3$ and MeOH (from 100% to 50% of MeOH in $CHCl_3$, 350 mL total volume) in a silicagel 60 column (3.0 × 45 cm, 0.063–0.200 nm, Merck K, Damstadt, Germany). The resultant fraction, SE-S7 (287 mg), showing higher anti-AChE activity (Fig. 1c) was further purified in a Sephadex LH-20 column (2.5 × 30 cm, 25–100 mesh, GE Healthcare Bio-Sciences AB, Uppsala, Sweden) with MeOH (850 mL) as a mobile phase to yield 7 subfractions (S7-L1, -L2, -L3, -L4, -L5, -L6, and -L7). Subsequently, the subfraction S7-L3 (90 mg), which showed higher anti-AChE activity (Fig. 1c), was further purified to yield the potential bioactive compound S7-L3-3 using high-performance liquid chromatography (HPLC) techniques.

2.2.2. HPLC conditions

HPLC experiments were performed using an Agilent HPLC instrument (Infinity 1260, CA, USA) with a 1260 quaternary pump, 1260 autosampler (ALS), 1260 diode-array detector (DAD), and 1260 thermostatted column compartment (TCC). The bioactive S7-L3-3 candidate was purified, by injecting S7-L3 into a Zorbax Eclipse XDB® C18 prep column (9.4 × 250 mm, 5 μm, Agilent Technologies) with a gradient eluent of acetonitrile and 0.04% trifluoroacetic acid at the retention time of 26.5 min. HPLC profiles and the UV spectrum (Fig. 1b) were recorded using an Agilent UV detector (1260 DAD, 190–400 nm, 20-nm step) at a 300 nm/reference 360 nm. The methanol-solubilized S7-L3 was also purified by a multiple preparative HPLC (LC-Forte, YMC, Kyoto, Japan) equipped with a Triart C18 prep column (20 × 250 mm, 5 μm, YMC, Kyoto, Japan) and a gradient eluent of MeOH and water to give a pure compound (S7-L3-3, 38.5 mg).

2.2.3. ESI-MS, ^{1}H-NMR and ^{13}C-NMR analysis

The isolated bioactive S7-L3-3 was characterized using ESI-MS, ^{1}H-NMR and ^{13}C-NMR techniques. ESI-MS was obtained in a liquid chromatography mass spectrometer (AGILENT 1100, Agilent Technologies,

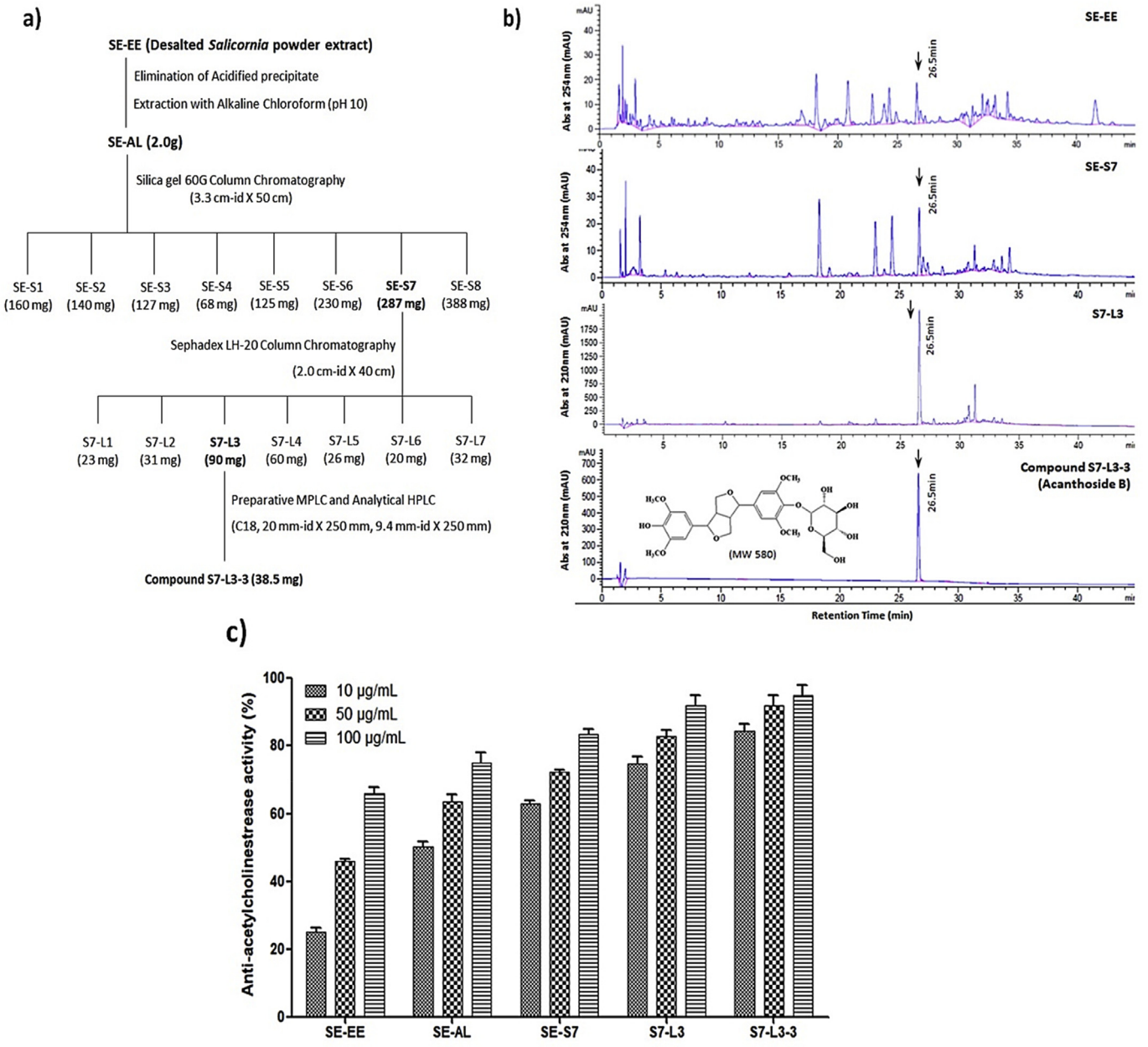

Fig. 1. Anti-AChE activity-guided isolation and chromatographic profiles of the active fractions/candidates from SE-EE: a) Schematic representation of the anti-AChE-guided isolation from SE-EE; b) representative HPLC chromatogram of active fractions/candidates acquired from the SE-EE; c) Anti-AChE activities of the isolated active fractions/candidates from the SE-EE.

USA) using both negative and positive modes. ^{1}H-NMR and ^{13}C-NMR spectra were measured on a Jeol instrument (^{1}H NMR at 600 MHz, ^{13}C-NMR at 150 MHz, JNM-ECA 600, Jeol, Japan) in DMSO-d_6.

2.3. Animals and treatment

Male C57BL/6N mice strains (8–9 weeks; 24–27 g) were procured from the Deahan Bio Link (Eumseong, Korea). All the animals were housed in a controlled environment (23 ± 1 °C; 50% ± 5% humidity; 12 h dark-light cycle) and allowed water and food *ad libitum*. After a week of acclimatization, the animals were randomly divided into experimental groups (n = 8 per group). The animal experimental study design is elucidated in Fig. 3c. In brief, the animals were divided into five groups - Control group (0.9% saline, *i.p.*), Scopolamine 2 mg/kg, (Scopolamine in 0.9% saline, *i.p.*), Aca.B 10 (Aca.B 10 mg/kg, *p.o.* + Scopolamine 2 mg/kg *i.p.*), Aca.B 20 (Aca.B 20 mg/kg, *p.o.* + Scopolamine 2 mg/kg *i.p.*) and Tacrine (10 mg/kg, *p.o.* + Scopolamine 2 mg/kg *i.p.*). Aca.B and tacrine were administered by oral gavage dissolved in 0.9% saline containing 1% Tween 80 and 0.9% saline, respectively, for 7 days prior to Scopolamine injection.

For the bioavailability studies, two groups of mice (n = 18 per group) were caged separately, where each group received a single 20 mg/kg dose of Aca.B either by oral gavage (*p.o*) or intraperitoneally (*i.p*). Subsequently, at different time points, i.e., 0 h, 0.5 h, 1 h, 3 h, 6 h and 24 h, the blood samples were collected by cardiac puncture, and the animals were euthanized to procure the brain samples. Then, both samples were processed appropriately and the blood and brain lysates were run through HPLC to determine the concentration of Aca.B in the samples. All the experiments were accomplished in accordance with the Principles of Laboratory Animal Care (NIH publication no.85-23, revised 1985) and approved by Konkuk University Institutional Animal care and Use Committee (KU17068).

2.4. Behavioral studies

2.4.1. Step-through passive avoidance test

The step-through passive avoidance test (PAT) was conducted using a Gemini active and passive avoidance instrument (San Diego Instruments, San Diego, CA) linked with a computerized system as described earlier (Govindarajan Karthivashan et al., 2018a,b), with slight modifications. In brief, on the day of acquisition, animals were individually habituated in the lighted compartment for 30 s, followed by a computer-operated opening of the guillotine door and holding of the trial for 300 s. On the entry of the animal to the dark compartment, the programmed door was automatically closed, after which the animal received a single low- intensity foot shock of 0.5 mA for 5 s, followed by recording of the time latencies (LT). Subsequently, the exact same procedure was performed on the next day to record the retention time, except for the shock punishment, however, the time taken for the animal to enter the dark compartment (LT) was recorded. The criterion for learning was taken as an increase in the LT on the retention trial compared to the acquisition trial.

2.4.2. Spontaneous alternation performance (Y-maze test)

The memory functioning and exploratory behaviors of the animals were determined using a spontaneous alternation Y-maze test as described previously (Govindarajan Karthivashan et al., 2018a,b). In brief, after 30 min of PAT experiments, the animals were naively introduced to one wing of the clean Y-maze and allowed to explore freely. The arm entry was considered when the hind paws of the animal were completely moved into the arm. When the animal entered three arms in a consecutive pattern, it was considered spontaneous alternation behavior on overlapping triplets. The total number of arm entries was recorded visually by a person unaware of the experimental groups. The percentage of alternation was calculated using the following formula.

$$\text{Percentage alternation} = [(\text{number of alternations}) / (\text{total number of arm entries} - 2)] \times 100$$

2.5. Tissue procurement and quantification of protein

An hour after the behavioral tests, the animals were anesthetized and euthanized. The whole brain was excised carefully from the skull and rinsed twice with ice-cold saline, followed by subsequent procurement of the hippocampus and cerebral cortex, as described earlier (Govindarajan Karthivashan et al., 2017). The excised hippocampi and/or cerebral cortex was subjected to AChE, antioxidant, and western blot analyses and ELISA. In brief, a portion of the tissue sample was homogenized using lysis buffer (Millipore) with a protease inhibitor cocktail (Roche, Mannheim, Germany) and the supernatants were stored at −70 °C for western blot analysis and the remaining portion was used for AChE and antioxidant analyses and ELISA. The protein level of the homogenates was quantified using a Bio-Rad DC Protein Assay kit according to the manufacturer's protocol and was then normalized for further analysis.

2.6. AChE activity

AChE activity in the homogenates of the hippocampus and cerebral cortex were determined using a Biochain kit (Biochain, CA) according to the manufacturer's procedure, as described earlier (Govindarajan Karthivashan et al., 2017). The absorbance was measured at 410 nm using a UV spectrophotometer.

2.7. Lipid peroxidation

The level of lipid peroxidation activity in the homogenates of the hippocampus was determined by measuring the level of malonaldehyde (MDA) generated using a lipid peroxidation colorimetric/fluorometric assay kit (BioVision, USA, CA) according to the manufacturer's procedure, as described earlier (Govindarajan Karthivashan et al., 2017). The absorbance was measured at 410 nm using a UV spectrophotometer.

2.8. SOD, CAT and GPx analyses

SOD, CAT and GPx activities of the tissue lysates were determined using Oxiselect superoxide dismutase, catalase assay kits (Cell Biolabs, Dan Diego, CA) and a glutathione peroxidase activity colorimetric assay kit (BioVision, USA, CA), respectively, according to the manufacturer's procedure, as described earlier (Govindarajan Karthivashan et al., 2018a,b). The absorbance of SOD, CAT and GPx activities were measured at 490 nm, 520 nm and 340 nm, respectively, using a UV spectrophotometer.

2.9. ELISA

The level of pro-inflammatory (TNF-α, IL-1β, IL-6) and anti-inflammatory (IL-10) cytokines in the hippocampus were quantified using commercially available ELISA kits (R&D systems, Minneapolis, MN) according to the manufacturer's procedure, as described earlier (Govindarajan Karthivashan et al., 2018a,b).

2.10. Western blot analysis

The protein level expressions of iNOS, COX-2, CREB/phospho-CREB and BDNF in the hippocampus were measured using western blot analysis as described in previously (Govindarajan Karthivashan et al., 2018a,b). In brief, the homogenates accumulated with equivalent proteins levels were separated in 10% polyacrylamide gels and transferred to PVDF membranes (Millipore, Bedford, MA, USA). Then, the membranes were blocked with 5% Bovine-serum Albumin (BSA) and subsequently incubated overnight at 4 °C with primary antibodies: anti-iNOS (1:2000), anti-COX-2 (1:2000), anti-CREB (1:1000), anti-*p*-CREB, (1:1000), anti-BDNF (1:1000) and anti-β-actin (1:1000). After 24 h, the membranes were washed and incubated with respective HRP-conjugated secondary antibodies (1:10000). The blots were visualized with a Davinch-Chemi & Fluoro Imaging System (Seoul, Korea), and their relative band densities were analyzed by ImageJ software (version-1.47).

2.11. Statistical analysis

All data were analyzed using GraphPad Prism, version 5.01 (La Jolla, CA, USA). The results were expressed as the mean ± SD and analyzed with a one-way ANOVA followed by Tukey's multiple comparison test. In this study, we compared the control group with the negative control group and, subsequently, the negative-control group with the treated and/or positive-control groups. In all cases, probability values of $p < 0.05$ were considered statistically significant.

3. Results

3.1. Anti-acetylcholinesterase (AChE) activity-guided purification from SE-EE

The crude SE-EE was subjected to ethanol precipitation and subsequently exposed to alkaline-chloroform solvent to yield 2 g of the SE-AL alkaloidal fraction. The SE-AL was then fractionated into 8 fractions (SE-S1 to SE-S8) using varied gradients of $CHCl_3$ and MeOH solvents (Fig. 1a), among which the SE-S7 fraction (287 mg) exhibited an enhanced anti-AChE potential of more than 80% at the evaluated higher concentration of 100 μg/mL (Supplementary fig. S1a-d). Subsequently, the SE-S7 fraction was further fractionated into 7 subfractions (S7-L1 to S7-L7) using MeOH as a mobile phase in a Sephadex LH-20 column,

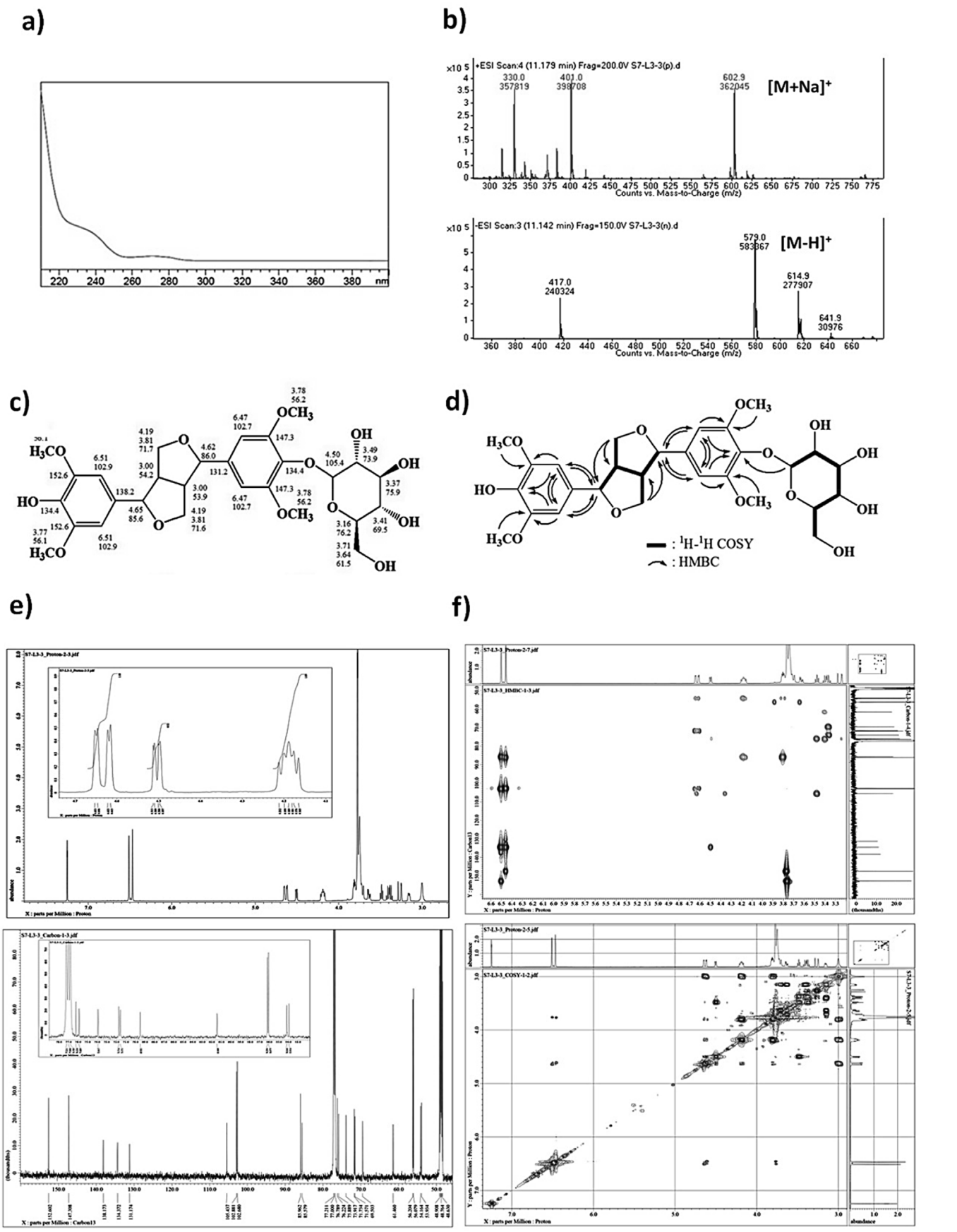

Fig. 2. Identification and characterization of the bioactive S7-L3-3: a) UV spectral profile of S7-L3-3; b) Negative and positive mode Electrospray ionization-mass spectrometry profiles of S7-L3-3; c), d) - Determined chemical structure of the isolated S7-L3-3 compound; proton and carbonyl resonances in the e) ^{1}H-NMR, ^{13}C-NMR and f) HMBC and (^{1}H–^{1}H COSY) spectra of S7-L3-3.

among which S7-L3 (90 mg) showed an enhanced anti-AChE potential of more than 85% at the evaluated higher concentration of 100 μg/mL (Supplementary fig. S2a-c). Finally, the bioactive S7-L3 was subjected to preparative and analytical HPLC columns to yield the pure bioactive candidate, S7-L3-3 (38.5 mg), which, when compared to its predecessor crude extracts/fractions, showed an enhanced anti-AChE potential of more than 90% at the evaluated higher concentration of 100 μg/mL (Fig. 1c). S7-L3-3 was observed at a retention time of 26.5 min and consistently appeared at the same retention time from the chromatographic profiles shown in Fig. 1b. Thus, this obtained bioactive S7-L3-3 candidate was further subjected to characterization.

3.2. Identification and characterization of the bioactive S7-L3-3

The UV spectrum of the major compound S7-L3-3 (MeOH, Agilent, 1200 DAD, 190–400 nm, 20-nm step) showed λ-maxima at 210 nm, 238 nm, and 272 nm, which are not characteristic of polyphenols and flavonoids (Fig. 2a). Further characterization of the compound S7-L3-3 white amorphous powder (10 mg) was conducted by ESI-MS, ^{1}H-NMR and ^{13}C-NMR analyses. The ESI-MS results, m/z 602.9 $[M+Na]^+$ and m/z 579.0 $[M-H]^+$, showed that the molecular weight of compound S7-L3-3 was 580 Da ($C_{28}H_{36}O_{13}$) (Fig. 2b). Compound S7-L3-3 was finally identified as acanthoside B (Syringaresinol 4′-O-β-glucopyranoside) by assignment of the proton and carbonyl resonances observed in the ^{1}H-NMR (Fig. 2e), ^{13}C-NMR (Fig. 2e), heteronuclear multiple bond correlation (HMBC) and correlated spectroscopy (^{1}H–^{1}H COSY) spectra (Fig. 2d and Fig. 2f). ^{1}H-NMR (600 MHz, $CDCl_3$) ppm: d 6.47 (2H, s, H-2 and H-6), 4.62 (1H, d, *J* 4.6 Hz, H-7), 3.00 (1H, m, H-8), 3.81 (1H, m, H-9a), 4.19 (1H, m, H-9b), 6.51 (2H, 1H, H-2′ and H-6′), 4.65 (1H, H-7′), 4.50 (1H, H-1″), 3.49 (1H, H-2″), 3.37 (1H, H-3″), 3.41 (1H, H-4″), 3.16 (1H. H-5″), 3.71 (1H, H-6″a), 3.64 (1H, H-6″b), 3.77 (6H, s, 2-OCH3), 3.78 (6H, s, 2-OCH3); ^{13}C-NMR ($CDCl_3$, 150 MHz) ppm: d131.2 (C-1), 102.3 (C-2), 147.3 (C-3), 134.4 (C-4), 147.3 (C-5), 102.7 (C-6), 86.0 (C-7), 53.9 (C-8), 71.6 (C-9), 56.1 (2 X–OCH3), 56.2 (2 Y–OCH3), 138.2 (C-1′), 102.9 (C-2′), 152.6 (C-3′), 134.4 (C-4′), 152.6 (C-5′), 102.9 (C-6′), 85.6 (C-7′), 54.2 (C-8′), 71.7(C-9′), 105.4 (C-1″), 73.9 (C-2″), 75.9 (C-3″), 69.5 (C-4″), 76.2 (C-5″), and 61.5 (C-6″).

3.3. Bioavailability kinetic studies of Aca.B in the blood and brain of mice

The mean blood and brain concentration-time profiles (i.e., 0 h, 0.5 h, 1 h, 3 h, 6 h and 24 h) of Aca.B in mice following *p.o.* and *i.v.* administration at a dose of 20 mg/kg are shown in Fig. 3a and Fig. 3b, respectively. The calibration curves showed good linearity over the concentration range of 0–320 μg/mL of Aca.B for the blood ($y = 25.821x + 28.04$) and brain ($y = 23.267x + 24.35$) studies with a correlation coefficient (R^2) value of 0.999 (Supplementary fig. S3a and fig. S3b). From Fig. 3a., both the *p.o.* and *i.v.* administration of Aca.B showed the highest concentration of Aca.B at 6 h in the blood, and from Fig. 3b, the maximum distribution of Aca.B in the brain tissue was attained at 24 h. Interestingly, both routes of administration showed a declining phase of Aca.B concentrations in the blood after 6 h and a relatively increasing trend in the brain tissues, indicating the considerable bioavailability of Aca.B in the brain tissue within 6–24 h.

3.4. Aca.B attenuated scopolamine-induced cognitive and behavioral impediments in mice

In the PAT experiments, during the acquisition session, all the groups of experimental animals exhibited a nonsignificant pattern of step-through latency times. During the retention phase, the scopolamine-administered mice exhibited a reduced latency time of 90.12 ± 28 s, compared to the control group of 300 s. The Aca.B-treated animals showed an improved trend in the latency times, which were significantly ($p < 0.05$) higher than those of the scopolamine-treated group (Fig. 3d). Precisely at the evaluated higher dose of 20 mg/kg of b.w., Aca.B substantially restored the latency time to 286 ± 26 s and this was close to the positive control group, the tacrine (10 mg/kg of b.w) group, at 290 ± 19 s.

In the case of Y-maze experiments, the results showed that the spontaneous alternation percentage for the scopolamine-treated animals were significantly ($p < 0.05$) decreased, with a value of 24.83 ± 3.76%, compared to the control groups at 78.5 ± 5.24%. Interestingly, at the assessed higher dose of 20 mg/kg of b.w., Aca.B significantly increased the spontaneous alternation percentage in scopolamine treated animals with a value of 67.33 ± 3.01%, and this was found proximal to the positive control tacrine-treated groups of 68.16 ± 3.81% (Fig. 3e). However, in the case of total arm entries, though scopolamine-treated mice showed a decreased number of total arm entries, treatment groups did not exhibit any significant changes in total arm entries (Fig. 3f).

3.5. Anti-AChE potential of Aca.B in the hippocampus and cortical regions of scopolamine administered mice

The endogenous AChE levels were measured in the hippocampal and cortical homogenates of the treated mice. As shown in Fig. 4a and Fig. 4b, the scopolamine-administered mice had significantly ($p < 0.05$) elevated the levels of AChE in both the hippocampus and cortical regions with the values of 31.50 ± 0.62 U/mg protein and 29.05 ± 1.67 U/mg protein, respectively, compared to the control groups, with values of 13.38 ± 0.62 U/mg protein and 13.87 ± 0.96 U/mg protein, respectively, while the Aca.B-treated groups exhibited a substantial dose-dependent decrease of AChE levels in both hippocampus and cortical regions compared to the scopolamine-treated group. At the evaluated high dose of 20 mg/kg of b.w, Aca.B significantly ($p < 0.05$) reduced the AChE levels by a nearly onefold decrease in both the hippocampus and cortical regions with the values of 21.20 ± 1.02 U/mg protein and 19.06 ± 0.21 U/mg protein, respectively, compared to the scopolamine-administered animals. It is also noteworthy that the anti-AChE activity of Aca.B is comparable to that of the tacrine-treated groups, which exhibited a nearly 1.5-fold decrease, with values of 15.34 ± 1.20 U/mg protein and 14.65 ± 1.50 U/mg protein, in both the hippocampus and cortical regions, respectively.

3.6. Anti-lipid peroxidation and antioxidant potential of Aca.B in the hippocampus of scopolamine-administered mice

As for lipid peroxidation activity, the endogenous MDA level in the tissue homogenates of the hippocampi was measured. From Fig. 4c, scopolamine-administered mice groups showed a significant ($p < 0.05$) increase in the MDA levels, with a value of 36.50 ± 4.66 nmol/mg protein, compared to the control group at 13.51 ± 3.19 nmol/mg protein. Subsequently, Aca.B-treated mice showed a significant ($p < 0.05$) suppression of the MDA level in the mice hippocampus in a dose-dependent fashion. Precisely, at the evaluated higher dose of 20 mg/kg of b.w, Aca.B significantly ($p < 0.05$) suppressed the MDA levels with a value of 19.95 ± 4.93 nmol/mg protein compared to the scopolamine-treated animals and was also found to be similar to the positive control tacrine-treated group, with a value of 15.57 ± 4.58 nmol/mg protein.

To determine the antioxidant potential, the endogenous antioxidant enzyme levels of SOD, CAT and GPx were measured in the tissue homogenates of the hippocampi. From Fig. 4d–f, overall, the scopolamine-administered mice substantially ($p < 0.05$) decreased the levels of antioxidant enzymes SOD, CAT, and GPx in the hippocampus, with values of 24.93 ± 2.84, 487.35 ± 24.24, and 16.49 ± 3.32 U/mg protein, compared to the control group, which exhibited values of 40.13 ± 5.29, 604.03 ± 38.02, and 27.17 ± 2.91 U/mg protein, respectively. However, a dose-dependent increase in the level of these antioxidant enzymes was observed in the Aca.B-treated groups. Indeed,

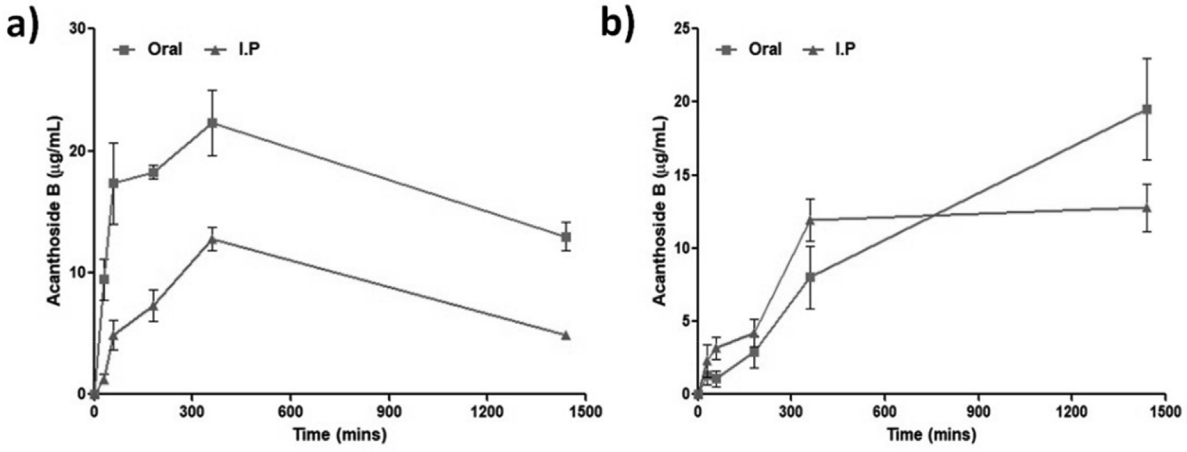

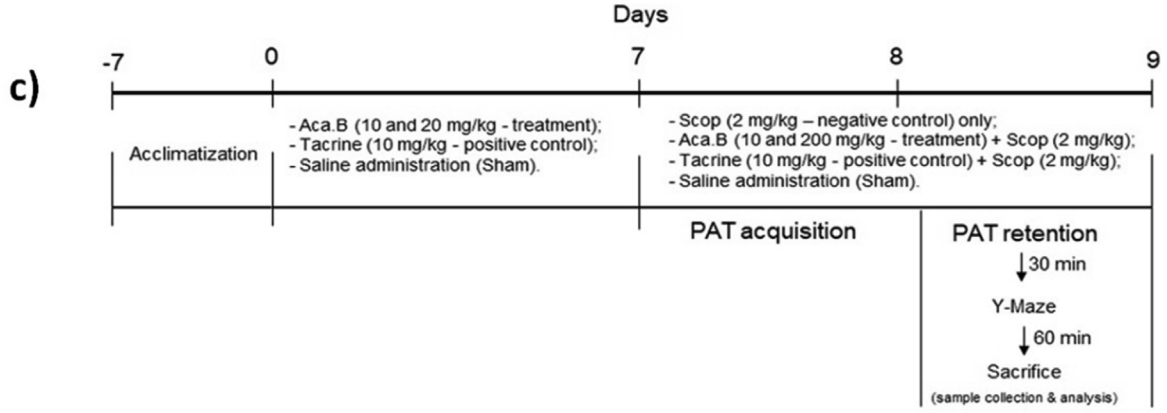

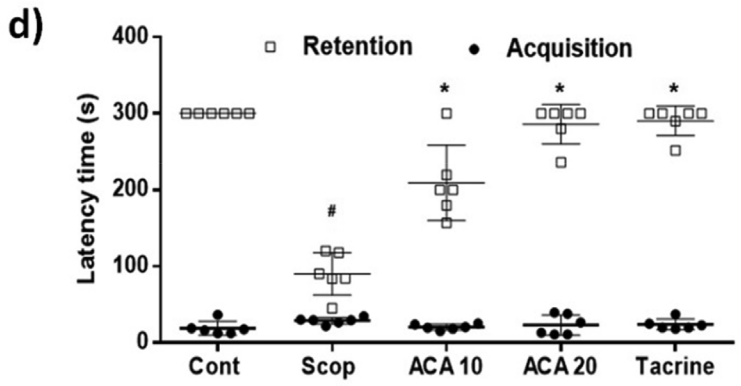

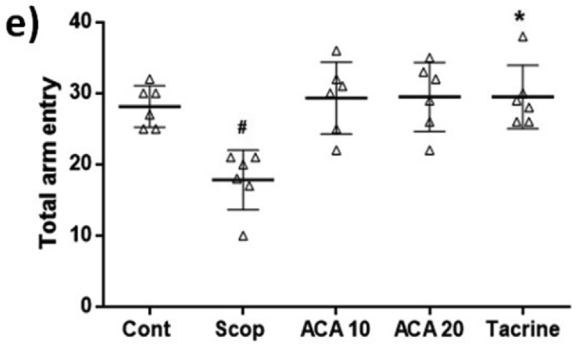

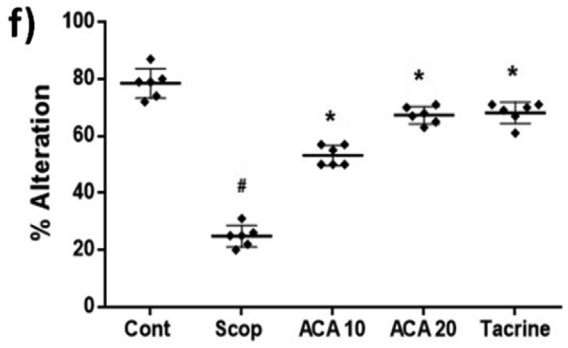

(caption on next page)

Fig. 3. Effects of Aca.B on scopolamine-inflicted cognitive and behavioral impairment in C57/BL6N mice: The pharmacokinetic profiles of Aca.B in the a) blood and b) brain of the orally and intraperitoneally administered mice; c) schematic representation of the animal experimental design; d) In the step-through passive avoidance test, the latency variance in the acquisition and retention phase was acquired; In the spontaneous alternation performance (Y-maze test), e) the total arm entry and f) percentage of alternation was acquired. Data are expressed as the mean ± SD (n = 6). One-way ANOVA-Tukey's multiple comparison test was performed. #: $p < 0.05$ compared with the control group; *: $p < 0.05$ other treated groups compared with the scopolamine group. Con-Control; Scop-Scopolamine; Tac-Tacrine.

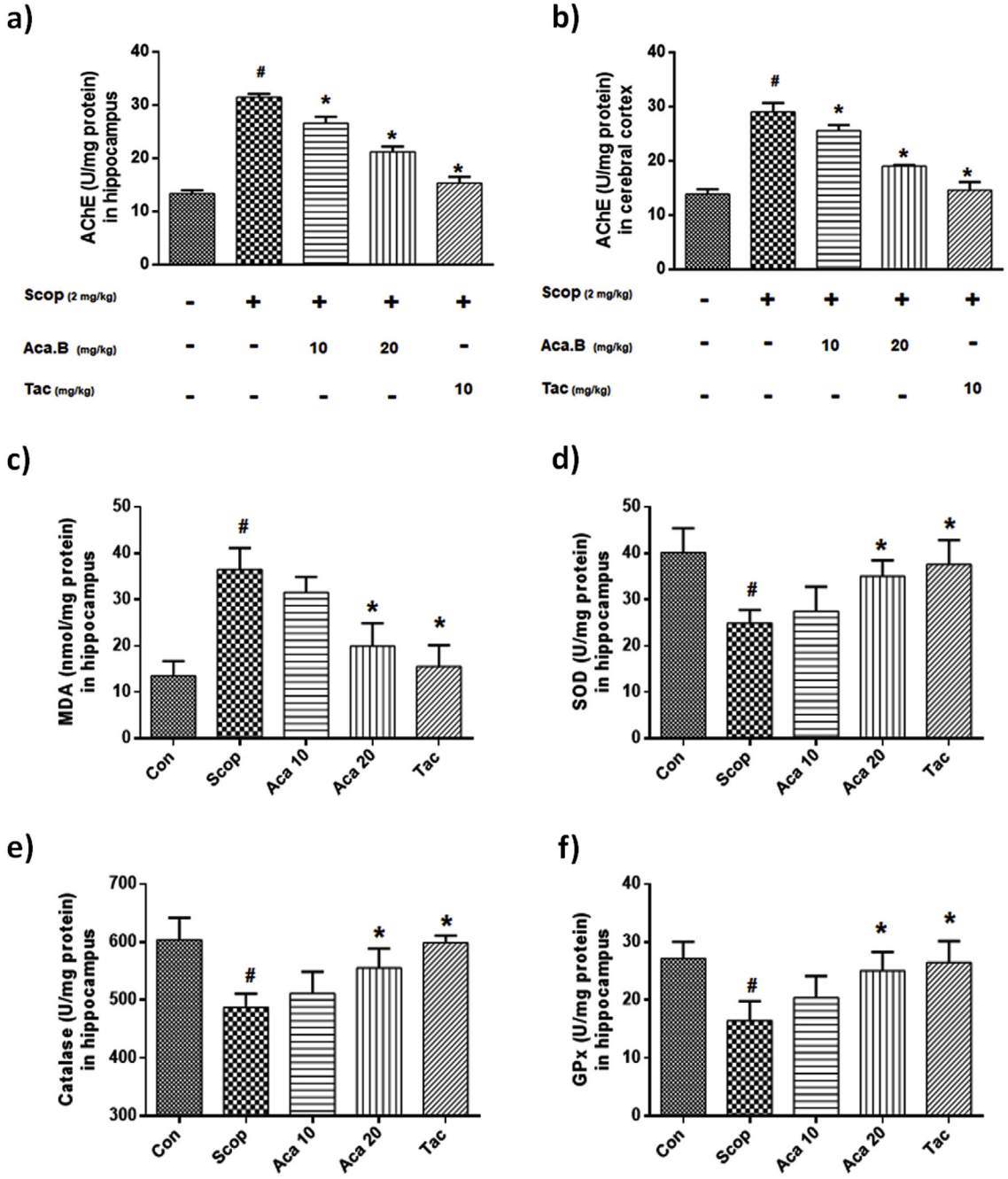

Fig. 4. Effects of Aca.B on scopolamine-inflicted cholinergic impairment, lipid peroxidation and endogenous antioxidant levels in C57/BL6N mice: AChE activity - a) AChE levels in the hippocampus, b) AChE levels in the cerebral cortex. Tacrine (10 mg/kg) was used as a positive control; Endogenous levels of oxidative stress/antioxidant enzymes - c), d), e) and f) represents the lipid peroxidation (MDA), superoxide dismutase (SOD), catalase (CAT) and glutathione peroxidase (GPx) levels in the hippocampus, respectively. The data are expressed as the mean ± SD (n = 5, pooled biological replicates). One-way ANOVA-Tukey's multiple comparison test was performed. #: $p < 0.05$ compared with the control group; *: $p < 0.05$ other treated groups compared with the scopolamine group. Con-Control; Scop-Scopolamine; Tac-Tacrine.

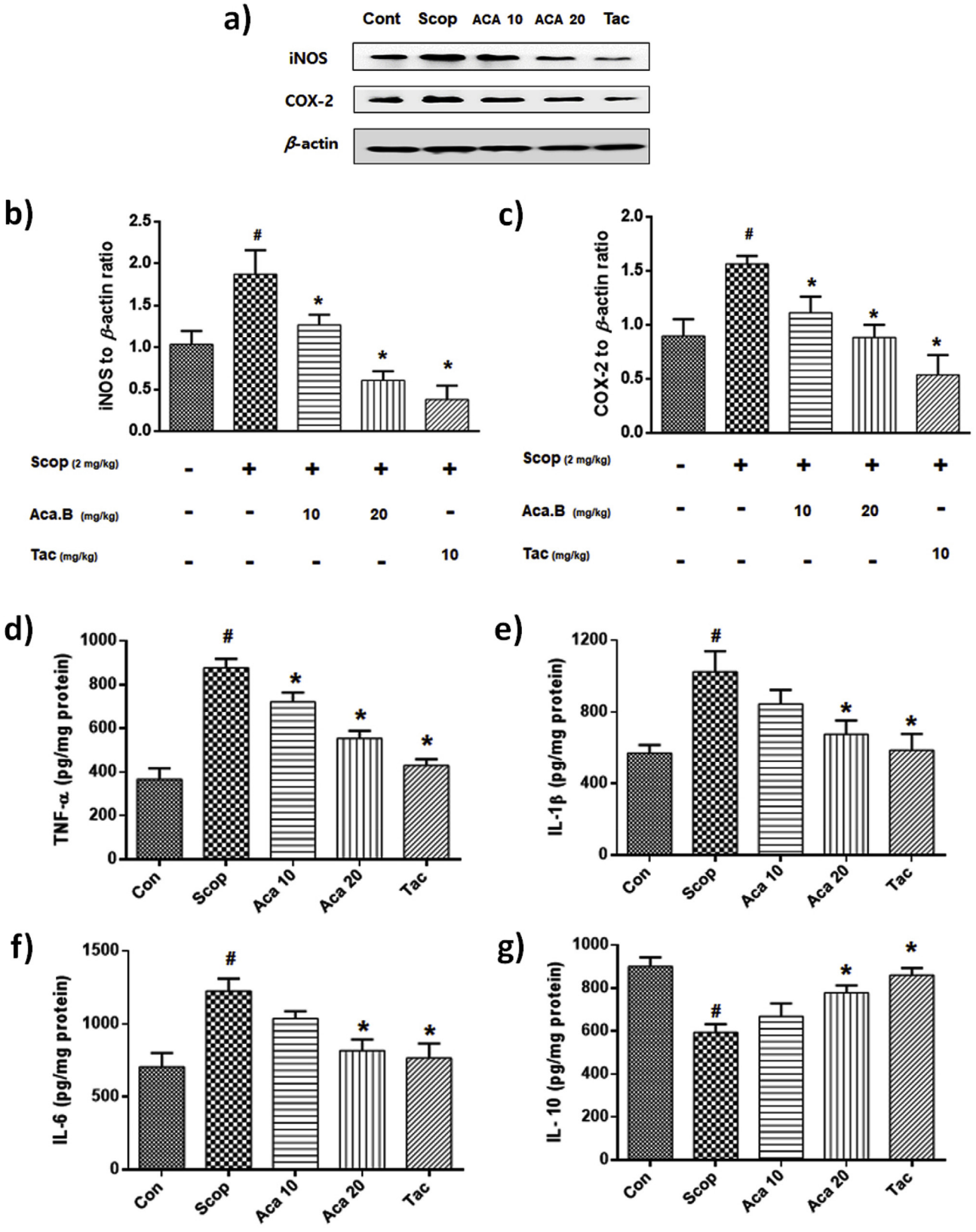

Fig. 5. Effects of Aca.B on scopolamine inflicted neuroinflammation in C57/BL6N mice: a) iNOS and COX-2 protein expressions in the hippocampus (n = 3) was determined by western blotting analysis, and b), c) represents the quantification of inflammatory protein expression relative to β-actin, which was achieved using ImageJ software; d), e), f) and g) represent the levels of TNF-α, IL-1β, IL-6 and IL-10 proteins in the hippocampus (n = 5, pooled biological replicates), respectively, as acquired via an ELISA. Data are expressed as the mean ± SD. A one-way ANOVA-Tukey's multiple comparison test was performed. #: $p < 0.05$ compared with the control group; *: $p < 0.05$ other treated groups compared with the scopolamine group. Con-Control; Scop-Scopolamine; Tac-Tacrine.

at the evaluated higher dose of 20 mg/kg of b.w, Aca.B significantly ($p < 0.05$) elevated the level of antioxidant enzymes SOD, CAT and GPx in the hippocampus, with values of 35.06 ± 3.46, 555.38 ± 33.87 and 25.08 ± 3.24 U/mg protein, compared to the scopolamine-treated group. It was proximal to the tacrine-treated positive control group, with values of 37.59 ± 5.29, 598.87 ± 12.77 and 26.48 ± 3.71 U/mg protein, respectively.

3.7. Anti-neuroinflammatory potential of Aca.B in the hippocampus of scopolamine-administered mice

Neuroinflammation is one of the major clinical hallmarks of several neurodegenerative disorders, including AD. To determine the anti-neuroinflammatory potential of Aca.B, we evaluated modulations in the protein level expressions of the inflammatory mediators iNOS and COX-2 using western blot analysis and the level of pro- (TNF-α, IL-1β, IL-6) and anti- (IL-10) inflammatory cytokine expression using ELISA kits in the hippocampi of Aca.B-treated scopolamine-inflicted mice. From Fig. 5a – c, the western blot results showed that scopolamine-administered mice exhibited significant ($p < 0.05$) elevation in the protein expression of iNOS and COX-2, which was approximately 1.5-fold higher than that of the control groups. In accordance, the ELISA results (Fig. 5d–g) of scopolamine-administered mice showed a significant ($p < 0.05$) increase in TNF-α, IL-1β, and IL-6 and a decrease in IL-10 levels, with values of 876.71 ± 41.76 pg/mg protein, 1025.75 ± 114.34 pg/mg protein, 1226.50 ± 84.29 pg/mg protein and 594.57 ± 37.93 pg/mg protein compared to the control group with the values of 376.02 ± 51.28 pg/mg protein, 570.25 ± 45.50 pg/mg protein, 705.00 ± 96.07 pg/mg protein and 900.97 ± 42.61 pg/mg protein, respectively. Conversely, from Fig. 5a–g, Aca.B-treated animals dose-dependently suppressed the level of pro-inflammatory mediators and the cytokine levels of expression and showed a significant elevation in the level of anti-inflammatory cytokine expressions. Indeed, at the evaluated higher dose of 20 mg/kg of b.w, Aca.B exhibited approximately 1.5- to 2-fold suppression of iNOS and COX-2 expression compared to the scopolamine-treated groups and was found to be proximal to the untreated and tacrine-treated groups (Fig. 5a–c). Interestingly, the higher dose of Aca.B also significantly suppressed the TNF-α, IL-1β, and IL-6 levels and increased the IL-10 levels, with values of 554.98 ± 33.41 pg/mg protein, 675.00 ± 78.17 pg/mg protein, 817.60 ± 76.45 pg/mg protein and 779.14 ± 33.43 pg/mg protein, respectively, and was found to be similar to the tacrine-treated positive control groups, with values of 430.43 ± 28.43 pg/mg protein, 586.37 ± 90.69 pg/mg protein, 765.00 ± 76.45 pg/mg protein and 779.14 ± 33.43 pg/mg protein, respectively.

3.8. Regulatory effects of Aca.B on the TrkB/CREB/BDNF pathway in the hippocampus of scopolamine-administered mice

TrkB/BDNF/CREB is a prominent molecular pathway precisely involved in the survival of neurons and neurogenesis. Based on the promising evidence of anti-AChE, antioxidant and anti-neuroinflammatory potential of Aca.B, we further extended our investigation to study its impact on the TrkB/CREB/BDNF pathway in a scopolamine-inflicted mouse model. In accordance, the protein levels of TrkB/*p*-TrkB, BDNF and CREB/*p*-CREB in the mice hippocampi were determined with western blot analysis. As seen in Fig. 6a – e, as anticipated, the scopolamine-administered mice mildly suppressed the protein expressions of *p*-TrkB, BDNF and *p*-CREB and was found to be nonsignificant compared to the control group. However, the Aca.B-treated group dose-dependently elevated the protein expression of neurotropic factors in scopolamine-administered mice. Indeed, the evaluated higher dose of Aca.B at 20 mg/kg of b.w significantly ($p < 0.05$) increased the *p*-TrkB, BDNF and *p*-CREB expression by approximately 1–1.5-fold higher than that of the scopolamine-treated animals. Interestingly, the increase in *p*-TrkB, BDNF and *p*-CREB protein expression were found to be comparable to that of the positive control, tacrine-treated group.

4. Discussion

Salicornia europaea L. (SE) is a halophytic plant species that is commonly utilized as a salt-substitute or as a fermented food supplement in Korea and other coastal regions of East Asia (Kang et al., 2015; Seo et al., 2010). The plant possesses several bioactive secondary metabolites; i.e., phenolic compounds, flavonoids, alkaloids, tannins, sterols and saponins, which sequentially have been attributed to its multitherapeutic potential against various chronic clinical conditions, i.e., diabetes, hyperlipidemia, tumor invasion, vascular neointima, oxidative stress and adipogenesis (Hwang et al., 2010; Kang et al., 2015; Park et al., 2006; Patel, 2016). Recently, our research team determined the neuroprotective potential of SE-EE against a scopolamine-inflicted mouse model (Govindarajan Karthivashan et al., 2018a,b). It is also noteworthy that, recently, the SE-EE has successfully entered the clinical trial phase in Seoul National University Hospital, Korea (Yonhap News agency, n.d.). However, the potential active compound responsible for its elite neuroprotective activity was not deciphered yet. Thus, as an extension of our previous work, in this study, we systematically identified and characterized the potential effective compound of SE-EE and, also, we investigated the anti-cholinergic, antioxidative, anti-neuroinflammatory and anti-amnesic potential of the same.

AD is a multifaceted neurodegenerative complication that primarily accounts for up to 75% of worldwide cases of dementia in an aging population (Fiest et al., 2016). AD is clinically characterized by cognitive decline and memory loss associated with behavioral and psychological disturbances (Fiest et al., 2016; Scheltens et al., 2016). However, the pathophysiology of AD involves several sequestered complications, i.e., cholinergic impediments, oxidative stress, neuroinflammation, prion-protein trafficking and progressive neuronal degeneration, which are responsible for cognitive decline and memory loss, mostly in the cortical and hippocampal regions of the brain (Canter et al., 2016; Salim, 2017). As cholinergic impairment is one of the clinical hallmarks of AD pathology, we initially screened the fractions/subfractions obtained from SE-EE based on *in vitro* anti-AChE activity, as reported in previous studies (Dastmalchi et al., 2009; Jung and Park, 2007). Dastmalchi K et al. reported that rosmarinic acid and its isomers from *Melissa officinalis* L. extract showed highly potent AChE inhibitory activity, and Jung M et al. showed that, among several isolated candidates of *Agrimonia pilosa* L. extract, the quercetin flavonoid exhibited potent AChE inhibitory activity, which could possibly be attributed to their neuroprotective potential, respectively (Dastmalchi et al., 2009; Jung and Park, 2007). Until now, AChE inhibitors have been one of the major classes of drugs currently used for the treatment of AD dementia. The existing Food and Drug Administration (FDA) approved AChE inhibitors, galantamine and rivastigmine, are alkaloids, among which galantamine is the only naturally occurring substance (Dos Santos, Gomes, Pinto, Camara and Paes, 2018; Ng et al., 2015; Vrancheva et al., 2016). Thus, we aimed to isolate new AChE inhibitory alkaloid compounds from SE-EE. We primarily prepared a crude alkaloidal fraction, SE-AL, using repeated acid precipitation and alkaline solvent extraction of SE-EE and screened various subfractions separated by polarity and molecular size-based column chromatography of SE-AL. Of the finally purified candidates, S7-L3-3 showed enhanced AChE inhibitory activity of more than 80% at a low concentration of 10 μg/ml. S7-L3-3 was then identified and characterized as Acanthoside B using NMR, UV, and ESI-MS spectral analyses.

Typically, botanical alkaloids are derived from amino acids and have nitrogen in a heterocyclic ring; however, Aca.B, also called syringaresinol- 4′-O-β-glucopyranoside, was found to be a protoalkaloid compound that was derived from amino acids but did not have nitrogen in a heterocyclic ring (Fig. 2c and d). The protoalkaloid compound acanthoside B, which is composed of 4 methoxyl phenyl rings and two

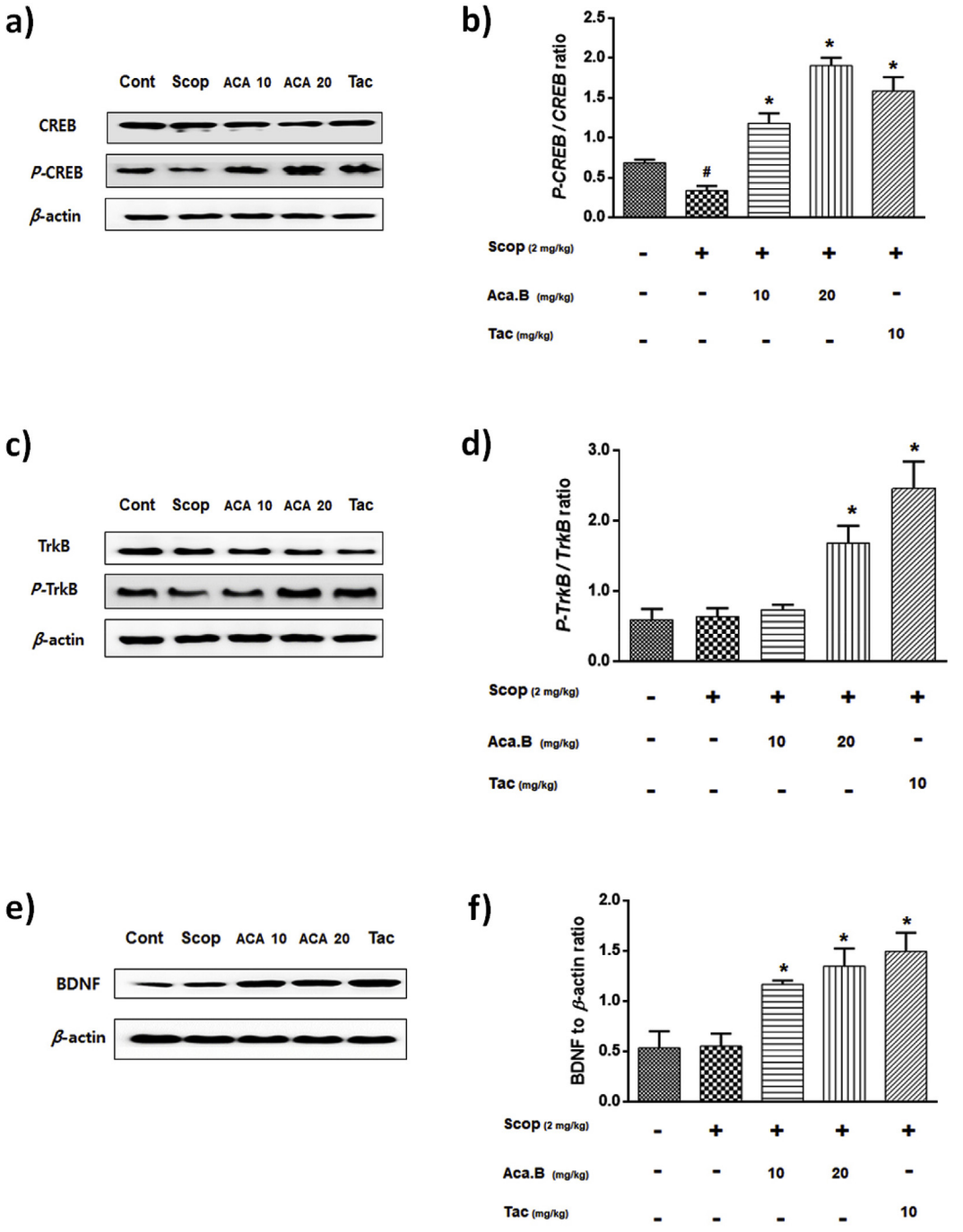

Fig. 6. Effects of Aca.B on TrkB/CREB/BDNF signaling in the hippocampus of C57/BL6N mice: a), c) and d) shows the immunoblots of CREB, *p*-CREB, TrkB, *p*-TrkB and BDNF protein expression in the hippocampus (n = 3), respectively, as determined via western blotting; b), d) and f) represent the quantification of protein expression relative to β-actin or phosphorylated proteins using ImageJ software. The data are expressed as the mean ± SD. #: $p < 0.05$ compared with the control group; *: $p < 0.05$ other treated groups compared with the scopolamine group. Con-Control; Scop-Scopolamine; Tac-Tacrine.

hexahydrofuroxanes, has been isolated as a constituent from the root and bark of some plants (Cao and Qi, 1993; Liu et al., 2010). Excluding a paper that mentions Aca.B as a constituent in lung inflammation-inhibitory *Acanthopanax divaricatus* extract (J. H. Lee, Sun, Kim, Lee and Kim, 2016), very few studies have reported its physiological and biological activities. Interestingly, there is a report that Aca.B was detected in rat plasma by HPLC-MS/MS after oral administration of *Acanthopanax sessiliflorus* fruit extract (Du et al., 2016), and this result is in agreement with our bioavailability kinetic studies of Aca.B. These results indicated that the hydrophobic nature of methoxyl-phenyl ring in acanthoside B has helped it pass through the biological membrane.

In the case of *in vitro* studies in LPS stimulated BV-2 microglial cells, the treatment of Aca.B did not exhibit substantial toxicity even at the higher dose of 500 μg/mL, however, Aca.B dose-dependently suppressed the LPS-induced nitric oxide production (Supplementary fig. S4a and fig. S4b). Thus, based on the *in vitro* anti-AChE potency and nitric oxide inhibitory activities of Aca.B, we further extended our investigation on evaluating the therapeutic potential of Aca.B in a scopolamine-induced amnesic AD-like mouse model by using 1% of tween 80 as a vehicle solvent for Aca.B. Being a single pure compound, we opted the Aca.B doses of 10 and 20 mg/kg of animal *b.w.* for the further animal investigations. Initially, the kinetics-based biodistribution

studies of Aca.B (20 mg/kg of b.w) showed that the oral route of administration exhibited relatively substantial bioavailability (6–24 h) in both the blood and brains of the treated mice compared to intraperitoneal administration. This was found to be in harmony with the previous pharmacokinetic data of Aca.B in rat plasma, where oral administration showed relatively higher bioavailability than intravenous administration (Du et al., 2016). Thus, the same route of administration was employed for further therapeutic investigations in mice. Scopolamine, an acetylcholine receptor agonist, is well documented to inflict cognitive and behavioral deficits in animals, particularly in spatial learning and memory (Ennaceur and Meliani, 1992; Naghdi et al., 2006; Saraf et al., 2011). Being an agonist of the ACh receptor, scopolamine administration substantially interrupts the postsynaptic transmission of ACh and, in turn, augments AChE activity by facilitating the hydrolysis of available ACh (Tota et al., 2012). Thus, this classic amnesic AD-like animal model was adapted for this study. As anticipated, here, scopolamine administration inflicted behavioral and cognitive deficits in mice, accompanied by elevated AChE activity in the hippocampal and cortical regions, which was effectually withdrawn by Aca.B. Previously, Csernansky et al. reported that AChE inhibitors, i.e., physostigmine, donepezil and galantamine, ameliorated the behavioral deficits in an MK-801-inflicted mouse model (Csernansky et al., 2005). Subsequently, another research team also reported that AChE inhibitors, i.e., physostigmine and donepezil, effectually overcame the behavioral deficits in Tg2576 AD transgenic mice (Dong et al., 2005). Inhibition of AChE activity enhanced the basal dendritic long-term potentiation in the hippocampal regions of the brain, thereby potentially alleviating the cognitive and behavioral impediments (Doralp and Leung, 2008). It is also noteworthy that, until now, AChE inhibitors have been considered as potentially one of the most useful therapeutic strategies in the clinical management of mild to moderate AD patients (Raina et al., 2008). In accordance, in this study, Aca.B effectually suppressed the AChE activity in the hippocampal and cortical regions of the brain and thereby attenuated the cognitive and behavioral impediments induced by scopolamine.

Despite AD being a multifaceted complication, as discussed earlier, the altered antioxidant system based oxidative stress and hyperactive glial cells mediated neuroinflammation were also suggested to play significant roles in the etiology and progression of the neurodegenerative conditions (Agostinho et al., 2010). Indeed, accumulating evidence has shown elevated lipid peroxidation activities and detrimental effects on the endogenous enzymatic and nonenzymatic antioxidants in the brains of AD patients, especially in the temporal lobe region (Palmer and Burns, 1994; Poprac et al., 2017; Swomley and Butterfield, 2015). Remarkably, scopolamine administration was also shown to mimic the deterioration of antioxidant systems in animals (Praticò, 2008). As reported earlier (J. Li et al., 2016; Rahnama et al., 2015), in this study, scopolamine administration substantially induced elevated MDA levels and decreased the pattern of endogenous antioxidant enzyme (SOD, CAT and GPx) levels in the mice. Interestingly, Aca.B treatment effectually suppressed the MDA levels and restored the endogenous antioxidant defense system in the scopolamine-intoxicated mouse brains. On the other hand, as reported in previous studies (Guo et al., 2016; B. Lee, Sur, Shim, Lee and Hahm, 2012), scopolamine administration significantly elevated the levels of pro-inflammatory mediators (iNOS and COX-2) and pro-inflammatory cytokines (TNF-α, IL-1β, and IL-6) in the hippocampal region of the mouse brains. However, prophylactic administration of Aca.B effectually downregulated these proinflammatory mediators and cytokines and dose-dependently increased the level of anti-inflammatory (IL-10) cytokines, which has been substantially reduced by scopolamine administration. This is found to be in agreement with previous study results (Govindarajan Karthivashan et al., 2018a,b; S.-P. Li et al., 2018; Saikia et al., 2018). Thus, Aca.B has shown substantial antioxidant and anti-neuroinflammatory potential in a scopolamine intoxicated mouse model.

Adult mammalian neurogenesis involves the production of new progenitor cells at the subgranular zone of hippocampal-dentate gyrus (DG) regions (Goncalves et al., 2016). Accumulating evidence has suggested that TrkB/CREB/BDNF signaling is one of the well-established pathways that facilitate neurogenesis (Y. Li et al., 2008; Numakawa et al., 2017). This vital process of producing new neurons in the DG regions plays a crucial role in improving spatial memory and cognitive reserve at the hippocampus. It is therefore involved in facilitating learning and memory processes in the adult mammalian brain (Y. Li et al., 2008; Murray and Holmes, 2011; Numakawa et al., 2017). In accordance, we further investigated the effects of Aca.B in the TrkB/CREB/BDNF signaling pathway. The molecular studies indicated that the scopolamine-administered mice showed reduced expression of *p*-TrkB, BDNF and *p*-CREB, which was effectually restored in the Aca.B-pretreated groups and was comparable with the positive control–tacrine treated groups. A previous study strongly suggested that the candidates that were able to activate the CREB/BDNF pathway showed an effectual neuroprotective potential (J. E. Lee et al., 2018; J. S. J. H. Lee et al., 2016a,b; C Lu et al., 2018a,b; Yoo et al., 2017). In addition, the activation of the BDNF and TrkB pathway had profound effects on improving cognition and elevated synaptic plasticity (Castello et al., 2014; Zeng et al., 2012). Accordingly, in this study, Aca.B was shown to improve the cognitive and behavioral performance in scopolamine-intoxicated mice by its anti-AChE potential and activation of the TrkB/CREB/BDNF signaling pathway.

5. Conclusions

This study demonstrated the neuroprotective effects of the bioactive Acanthoside B compound, which substantially attenuated scopolamine-inflicted AD-like amnesic traits by restoring the cholinergic activity, decreasing the endogenous antioxidant status, suppressing neuro-inflammation and activating the TrkB/CREB/BDNF pathway in mice, as with the desalted and enzyme-digested SE ethanol extract (SE-EE) of our previous works. This suggested that Aca.B likely contributes to the enhanced anti-amnesic activities of SE-EE and can be further developed as a potential drug candidate to treat neurodegenerative conditions.

Declaration of interests

The authors declare that they have no known competing financial interests or personal relationships that could have appeared to influence the work reported in this paper.

Author contributions

Govindarajan Karthivashan, conducted the animal experiments and wrote the manuscript. Shin-Young Park, Joon Soo Kim, aid in conducting animal-behavioral experiments. Mee-Hyang Kweon and Deuk-Hoi Kim conducted phyto-extraction, phytochemical analysis and associated writeups. Palanivel Ganesan provided valuable guidance and checked the manuscript flow and consistency. Dong-Kug Choi supervised the overall work and directed the final version of all contents. All authors reviewed and approved this manuscript.

Conflict of interest

The authors declare that there is no conflict of interest.

Acknowledgments

This research paper was supported by Konkuk University in 2018.

Appendix A. Supplementary data

Supplementary data to this article can be found online at https://doi.org/10.1016/j.fct.2019.04.062.

Transparency document

Transparency document related to this article can be found online at https://doi.org/10.1016/j.fct.2019.04.062.

References

Agostinho, P., Cunha, R.A., Oliveira, C., 2010. Neuroinflammation, oxidative stress and the pathogenesis of Alzheimer's disease. Curr. Pharmaceut. Des. 16 (25), 2766–2778.

Association, A., 2018. 2018 Alzheimer's disease facts and figures. Alzheimer's Dementia 14 (3), 367–429.

Bartolotti, N., Bennett, D.A., Lazarov, O., 2016. Reduced pCREB in Alzheimer's disease prefrontal cortex is reflected in peripheral blood mononuclear cells. Mol. Psychiatr. 21 (9), 1158.

Canter, R.G., Penney, J., Tsai, L.-H., 2016. The road to restoring neural circuits for the treatment of Alzheimer's disease. Nature 539 (7628), 187.

Cao, J.H., Qi, Y.P., 1993. [Studies on the chemical constituents of the herb huanghuaren (Sida acutá Burm. f.)]. Zhongguo Zhong Yao Za Zhi = Zhongguo Zhongyao Zazhi = China Journal of Chinese Materia Medica 18 (11), 681–682. 703. Retrieved from. http://www.ncbi.nlm.nih.gov/pubmed/8003231.

Castello, N.A., Nguyen, M.H., Tran, J.D., Cheng, D., Green, K.N., LaFerla, F.M., 2014. 7,8-Dihydroxyflavone, a small molecule TrkB agonist, improves spatial memory and increases thin spine density in a mouse model of Alzheimer disease-like neuronal loss. PLoS One 9 (3) e91453–e91453. https://doi.org/10.1371/journal.pone.0091453.

Csernansky, J.G., Martin, M., Shah, R., Bertchume, A., Colvin, J., Dong, H., 2005. Cholinesterase Inhibitors Ameliorate Behavioral Deficits Induced by MK-801 in Mice. Neuropsychopharmacology. vol. 30. Official Publication of the American College of Neuropsychopharmacology, pp. 2135–2143. https://doi.org/10.1038/sj.npp.1300761 12.

Dastmalchi, K., Ollilainen, V., Lackman, P., af Gennäs, G.B., Dorman, H.J.D., Järvinen, P.P., et al., 2009. Acetylcholinesterase inhibitory guided fractionation of Melissa officinalis L. Bioorg. Med. Chem. 17 (2), 867–871.

Dong, H., Csernansky, C.A., Martin, M.V., Bertchume, A., Vallera, D., Csernansky, J.G., 2005. Acetylcholinesterase inhibitors ameliorate behavioral deficits in the Tg2576 mouse model of Alzheimer's disease. Psychopharmacology (Berl) 181 (1), 145–152. https://doi.org/10.1007/s00213-005-2230-6.

Doralp, S., Leung, L.S., 2008. Cholinergic modulation of hippocampal CA1 basal-dendritic long-term potentiation. Neurobiol. Learn. Mem. 90 (2), 382–388. https://doi.org/10.1016/j.nlm.2008.05.013.

Dos Santos, T.C., Gomes, T.M., Pinto, B.A.S., Camara, A.L., Paes, A. M. de A., 2018. Naturally occurring acetylcholinesterase inhibitors and their potential use for Alzheimer's disease therapy. Front. Pharmacol. 9, 1192. https://doi.org/10.3389/fphar.2018.01192.

Du, P., Lei, M., Liu, Y., Yang, S., 2016. Simultaneous determination and pharmacokinetic study of six components in rat plasma by HPLC-MS/MS after oral administration of Acanthopanax sessiliflorus fruit extract. Int. J. Mol. Sci. 18 (1). https://doi.org/10.3390/ijms18010045.

Ennaceur, A., Meliani, K., 1992. Effects of physostigmine and scopolamine on rats' performances in object-recognition and radial-maze tests. Psychopharmacology (Berl) 109 (3), 321–330.

Fiest, K.M., Roberts, J.I., Maxwell, C.J., Hogan, D.B., Smith, E.E., Frolkis, A., et al., 2016. The prevalence and incidence of dementia due to Alzheimer's disease: a systematic review and meta-analysis. Can. J. Neurol. Sci. 43 (S1), S51–S82.

Godyń, J., Jończyk, J., Panek, D., Malawska, B., 2016. Therapeutic strategies for Alzheimer's disease in clinical trials. Pharmacol. Rep. 68 (1), 127–138. https://doi.org/https://doi.org/10.1016/j.pharep.2015.07.006.

Goncalves, J.T., Schafer, S.T., Gage, F.H., 2016. Adult neurogenesis in the Hippocampus: from stem cells to behavior. Cell 167 (4), 897–914. https://doi.org/10.1016/j.cell.2016.10.021.

Guo, C., Shen, J., Meng, Z., Yang, X., Li, F., 2016. Neuroprotective effects of polygalacic acid on scopolamine-induced memory deficits in mice. Phytomedicine 23 (2), 149–155. https://doi.org/https://doi.org/10.1016/j.phymed.2015.12.009.

Hwang, Y.P., Yun, H.J., Choi, J.H., Chun, H.K., Chung, Y.C., Kim, S.K., et al., 2010. 3-Caffeoyl, 4-dihydrocaffeoylquinic acid from Salicornia herbacea inhibits tumor cell invasion by regulating protein kinase C-δ-dependent matrix metalloproteinase-9 expression. Toxicol. Lett. 198 (2), 200–209.

Jung, M., Park, M., 2007. Acetylcholinesterase inhibition by flavonoids from Agrimonia pilosa. Molecules 12 (9), 2130–2139.

Kang, S., Kim, M.-R., Chiang, M., Hong, J., 2015. Evaluation and comparison of functional properties of freshwater-cultivated glasswort (Salicornia herbacea L.) with naturally-grown glasswort. Food Science and Biotechnology 24 (6), 2245–2250.

Karthivashan, G., Ganesan, P., Park, S.Y., Kim, J.S., Choi, D.K., 2018a. Therapeutic strategies and nano-drug delivery applications in management of ageing Alzheimer's disease. Drug Deliv. 25 (1), 307–320. https://doi.org/10.1080/10717544.2018.1428243.

Karthivashan, G., Park, S.-Y., Kim, J.-S., Cho, D.-Y., Ganesan, P., Choi, D.-K., 2017. Comparative studies on behavioral, cognitive and biomolecular profiling of ICR, C57BL/6 and its sub-strains suitable for scopolamine-induced amnesic models. Int. J. Mol. Sci. 18 (8), 1735.

Karthivashan, G., Park, S.-Y., Kweon, M.-H., Kim, J., Haque, M.E., Cho, D.-Y., et al., 2018b. Ameliorative potential of desalted Salicornia europaea L. extract in multi-faceted Alzheimer's-like scopolamine-induced amnesic mice model. Sci. Rep. 8 (1), 7174.

Kim, M.S., Seo, J.Y., Oh, J., Jang, Y.K., Lee, C.H., Kim, J.-S., 2017. Neuroprotective effect of halophyte Salicornia herbacea L. Is mediated by activation of heme oxygenase-1 in mouse hippocampal HT22 cells. J. Med. Food 20 (2), 140–151.

Lee, B., Sur, B., Shim, I., Lee, H., Hahm, D.H., 2012. Phellodendron amurense and its major alkaloid compound, berberine ameliorates scopolamine-induced neuronal impairment and memory dysfunction in rats. KOREAN J. PHYSIOL. PHARMACOL. 16 (2), 79–89. https://doi.org/10.4196/kjpp.2012.16.2.79.

Lee, J.E., Song, H.-S., Park, M.N., Kim, S.-H., Shim, B.-S., Kim, B., 2018. Ethanol extract of oldenlandia diffusa herba attenuates scopolamine-induced cognitive impairments in mice via activation of BDNF, P-CREB and inhibition of acetylcholinesterase. Int. J. Mol. Sci. 19 (2), 363. https://doi.org/10.3390/ijms19020363.

Lee, J.H., Sun, Y.N., Kim, Y.H., Lee, S.K., Kim, H.P., 2016b. Inhibition of lung inflammation by Acanthopanax divaricatus var. Albeofructus and its constituents. Biomolecules & Therapeutics 24 (1), 67–74. https://doi.org/10.4062/biomolther.2015.070.

Lee, J.S., Hong, S.S., Kim, H.G., Lee, H.W., Kim, W.Y., Lee, S.K., Son, C.G., 2016a. Gongjin-dan enhances hippocampal memory in a mouse model of scopolamine-induced amnesia. PLoS One 11 (8), e0159823. https://doi.org/10.1371/journal.pone.0159823.

Li, F., Gong, Q.-H., Wu, Q., Lu, Y.-F., Shi, J.-S., 2010. Icariin isolated from Epimedium brevicornum Maxim attenuates learning and memory deficits induced by d-galactose in rats. Pharmacol. Biochem. Behav. 96 (3), 301–305.

Li, J., Gao, L., Sun, K., Xiao, D., Li, W., Xiang, L., Qi, J., 2016. Benzoate fraction from Gentiana rigescens Franch alleviates scopolamine-induced impaired memory in mice model in vivo. J. Ethnopharmacol. 193, 107–116. https://doi.org/10.1016/j.jep.2016.08.001.

Li, S.-P., Wang, Y.-W., Qi, S.-L., Zhang, Y.-P., Deng, G., Ding, W.-Z., et al., 2018. Analogous β-carboline alkaloids harmaline and harmine ameliorate scopolamine-induced cognition dysfunction by attenuating acetylcholinesterase activity, oxidative stress, and inflammation in mice. Front. Pharmacol. 9, 346. https://doi.org/10.3389/fphar.2018.00346.

Li, Y., Luikart, B.W., Birnbaum, S., Chen, J., Kwon, C.-H., Kernie, S.G., et al., 2008. TrkB regulates hippocampal neurogenesis and governs sensitivity to antidepressive treatment. Neuron 59 (3), 399–412. https://doi.org/10.1016/j.neuron.2008.06.023.

Liu, W.-Y., Feng, F., Yu, C.-X., Xie, N., 2010. Qualitative and quantitative analysis of the main constituents of Radix Ilicis Pubescentis by LC-coupled with DAD and ESI-MS detection. Natural Product Communications 5 (1), 23–26. Retrieved from. http://www.ncbi.nlm.nih.gov/pubmed/20184013.

Lu, C., Wang, Y., Wang, D., Zhang, L., Lv, J., Jiang, N., et al., 2018a. Neuroprotective effects of soy isoflavones on scopolamine-induced amnesia in mice. Nutrients 10 (7). https://doi.org/10.3390/nu10070853.

Lu, C., Wang, Y., Xu, T., Li, Q., Wang, D., Zhang, L., et al., 2018b. Genistein ameliorates scopolamine-induced amnesia in mice through the regulation of the cholinergic neurotransmission, antioxidant system and the ERK/CREB/BDNF signaling. Front. Pharmacol. 9 (1153). https://doi.org/10.3389/fphar.2018.01153.

Min, A.Y., Doo, C.N., Son, E.J., Sung, N.Y., Lee, K.J., Sok, D.-E., Kim, M.R., 2015. N-palmitoyl serotonin alleviates scopolamine-induced memory impairment via regulation of cholinergic and antioxidant systems, and expression of BDNF and p-CREB in mice. Chem. Biol. Interact. 242, 153–162.

Murray, P.S., Holmes, P.V., 2011. An overview of brain-derived neurotrophic factor and implications for excitotoxic vulnerability in the Hippocampus. International Journal of Peptides 2011, 12. https://doi.org/10.1155/2011/654085.

Naghdi, N., Rezaei, M., Fathollahi, Y., 2006. Microinjection of ritanserin into the CA1 region of hippocampus improves scopolamine-induced amnesia in adult male rats. Behav. Brain Res. 168 (2), 215–220. https://doi.org/10.1016/j.bbr.2005.11.016.

Ng, Y.P., Or, T.C.T., Ip, N.Y., 2015. Plant alkaloids as drug leads for Alzheimer's disease. Neurochem. Int. 89, 260–270. https://doi.org/10.1016/j.neuint.2015.07.018.

Numakawa, T., Odaka, H., Adachi, N., 2017. Actions of brain-derived neurotrophic factor and glucocorticoid stress in neurogenesis. Int. J. Mol. Sci. 18 (11), 2312. https://doi.org/10.3390/ijms18112312.

Ower, A.K., Hadjichrysanthou, C., Gras, L., Goudsmit, J., Anderson, R.M., de Wolf, F., Initiative, for the A. D. N, 2018. Temporal association patterns and dynamics of amyloid-β and tau in Alzheimer's disease. Eur. J. Epidemiol. 33 (7), 657–666. https://doi.org/10.1007/s10654-017-0326-z.

Palmer, A.M., Burns, M.A., 1994. Selective increase in lipid peroxidation in the inferior temporal cortex in Alzheimer's disease. Brain Res. 645 (1), 338–342. https://doi.org/https://doi.org/10.1016/0006-8993(94)91670-5.

Park, S.H., Ko, S.K., Choi, J.G., Chung, S.H., 2006. Salicornia herbacea prevents high fat diet-induced hyperglycemia and hyperlipidemia in ICR mice. Arch Pharm. Res. (Seoul) 29 (3), 256.

Patel, S., 2016. Salicornia: evaluating the halophytic extremophile as a food and a pharmaceutical candidate. 3 Biotech 6 (1), 104.

Patterson, C., Lynch, C., Bliss, A., Lefevre, M., Weidner, M., 2018. World Alzheimer Report 2018 the State of the Art of Dementia Research: New Frontiers. Alzheimer's Disease International (ADI), London, pp. 1–42.

Poprac, P., Jomova, K., Simunkova, M., Kollar, V., Rhodes, C.J., Valko, M., 2017. Targeting free radicals in oxidative stress-related human diseases. Trends Pharmacol. Sci. 38 (7), 592–607. https://doi.org/https://doi.org/10.1016/j.tips.2017.04.005.

Praticò, D., 2008. Oxidative stress hypothesis in Alzheimer's disease: a reappraisal. Trends Pharmacol. Sci. 29 (12), 609–615. https://doi.org/https://doi.org/10.1016/j.tips.2008.09.001.

Rahnama, S., Rabiei, Z., Alibabaei, Z., Mokhtari, S., Rafieian-Kopaei, M., Deris, F., 2015. Anti-amnesic activity of Citrus aurantium flowers extract against scopolamine-induced memory impairments in rats. Neurol. Sci. 36 (4), 553–560. https://doi.org/10.1007/s10072-014-1991-2.

Raina, P., Santaguida, P., Ismaila, A., Patterson, C., Cowan, D., Levine, M., et al., 2008. Effectiveness of cholinesterase inhibitors and memantine for treating dementia:

evidence review for a clinical practice guideline. Ann. Intern. Med. 148 (5), 379–397.
Rhee, M.H., Park, H.-J., Cho, J.Y., 2009. Salicornia herbacea: botanical, chemical and pharmacological review of halophyte marsh plant. J. Med. Plants Res. 3 (8), 548–555.
Saikia, B., Barua, C.C., Sarma, J., Haloi, P., Tamuli, S.M., Kalita, D.J., et al., 2018. Zanthoxylum alatum ameliorates scopolamine-induced amnesia in rats: behavioral, biochemical, and molecular evidence. Indian J. Pharmacol. 50 (1), 30–38. https://doi.org/10.4103/ijp.IJP_417_17.
Salim, S., 2017. Oxidative stress and the central nervous system. J. Pharmacol. Exp. Ther. 360 (1), 201–205.
Saraf, M.K., Prabhakar, S., Khanduja, K.L., Anand, A., 2011. Bacopa monniera attenuates scopolamine-induced impairment of spatial memory in mice. Evid. Based Complement Altern. Med.: ECAM 2011, 236186. https://doi.org/10.1093/ecam/neq038.
Scheltens, P., Blennow, K., Breteler, M.M., de Strooper, B., Frisoni, G.B., Salloway, S., Van der Flier, W.M., 2016. Alzheimer's disease. Lancet 388 (10043), 505–517. https://doi.org/10.1016/s0140-6736(15)01124-1.
Seo, H., Jeon, B.Y., Yun, A., Park, D.H., 2010. Effect of glasswort (Salicornia herbacea L.) on microbial community variations in the vinegar-making process and vinegar characteristics. J. Microbiol. Biotechnol. 20 (9), 1322–1330.
Shal, B., Ding, W., Ali, H., Kim, Y.S., Khan, S., 2018. Anti-neuroinflammatory potential of natural products in attenuation of Alzheimer's disease. Front. Pharmacol. 9, 548. https://doi.org/10.3389/fphar.2018.00548.
Swomley, A.M., Butterfield, D.A., 2015. Oxidative stress in Alzheimer disease and mild cognitive impairment: evidence from human data provided by redox proteomics. Arch. Toxicol. 89 (10), 1669–1680. https://doi.org/10.1007/s00204-015-1556-z.
Tota, S., Hanif, K., Kamat, P.K., Najmi, A.K., Nath, C., 2012. Role of central angiotensin receptors in scopolamine-induced impairment in memory, cerebral blood flow, and cholinergic function. Psychopharmacology (Berl) 222 (2), 185–202. https://doi.org/10.1007/s00213-012-2639-7.
Van Dam, D., De Deyn, P.P., 2011. Animal models in the drug discovery pipeline for Alzheimer's disease. Br. J. Pharmacol. 164 (4), 1285–1300. https://doi.org/10.1111/j.1476-5381.2011.01299.x.
Vrancheva, R.Z., Ivanov, I.G., Aneva, I.Y., Dincheva, I.N., Badjakov, I.K., Pavlov, A.I., 2016. Alkaloid profiles and acetylcholinesterase inhibitory activities of Fumaria species from Bulgaria. Z. Naturforsch. C Biosci. 71 (1–2), 9–14. https://doi.org/10.1515/znc-2014-4179.
Yonhap News agency Bio-Venture Phyto “Development of Cognitive Functional Vegetable Material Development. n.d Retrieved from. https://en.yna.co.kr/view/AKR20180227162200017.
Yoo, J.-M., Lee, B.D., Sok, D.-E., Ma, J.Y., Kim, M.R., 2017. Neuroprotective action of N-acetyl serotonin in oxidative stress-induced apoptosis through the activation of both TrkB/CREB/BDNF pathway and Akt/Nrf2/Antioxidant enzyme in neuronal cells. Redox Biology 11, 592–599. https://doi.org/10.1016/j.redox.2016.12.034.
Zeng, Y., Liu, Y., Wu, M., Liu, J., Hu, Q., 2012. Activation of TrkB by 7,8-dihydroxyflavone prevents fear memory defects and facilitates amygdalar synaptic plasticity in aging. J. Alzheimer's Dis. 31 (4), 765–778. https://doi.org/10.3233/jad-2012-120886.